Effect of Acrylamide on Cerebral Neurons Development in Albino Rat

Ahmed A Allam [1,2]*, Manal Abdul-Hamid [2], Ahlam Bakry [2], Abdelwahb El-Ghareeb [3], Jamaan S Ajarem [1], Mohamed Sabri [4]

[1] King Saud University, College of Science, Zoology Department, Riyadh11451, Saudia Arabia.
[2] Department of Zoology, Faculty of Science, Beni-suef University, Egypt.
[3] Department of Zoology, Faculty of Science, Cairo University, Egypt.
[4] Oregon Health and Science University, Portland OR, USA.

Abstract: Acrylamide has been used to investigate the biochemical and morphological changes in developing rat cerebrum following exposure in pregnant rats. Non-anesthetized pregnant rats were given 10 mg/kg/day of acrylamide by gastric intubation. The pups were divided into 3 groups: Group A (control group); Group B (*prenatal exposure*); and Group C (*perinatal exposure*). Acrylamide-induced biochemical and morphological changes were studied in control and acrylamide-treated developing pups. Prenatal and perinatal acrylamide exposure significantly increased lipid peroxidation and reduced *glutathione* (GSH) and total thiol levels. Additionally, significant inhibition of peroxidase and *superoxide dismutase* (SOD) activities was observed in the developed cerebrum. Light microscopy revealed dramatic tissue changes. The nuclei in the cerebra of the acrylamide-treated groups exhibited significant decreases in nuclear DNA staining. In conclusion, acrylamide and its toxic metabolites induce malformations in the cerebra of neonatal rats from dams chronically exposed during gestation and lactation.

Introduction

There are numerous publications on the carcinogenic effects of acrylamide; however, there is little data on acrylamide-induced biochemical and morphological effects to the cerebrum during embryonic and postnatal development. Acrylamide is an industrial chemical used in the manufacture of polymers and synthetic organic chemicals. Polymeric acrylamide is used during filtration and flocculation in water treatment and waste processing industries and in mining and paper mills (Friedman, 2003). Acrylamide is metabolized to glycidamide by cytochrome P4502E1 (Dixit et al., 1982; Miller et al., 1982; Calleman et al., 1990; Sumner et al., 1992). Furthermore, acrylamide interacts with glutathione-S-transferase (GST) (Mukhtar et al., 1981; Das et al., 1982) to form N-acetyl-S-cysteine, which accounts for approximately 70% of the urinary acrylamide metabolites excreted in the rat (Sumner et al., 1997).

Acrylamide causes oxidative stress, and the effect is more apparent at high doses (Yousef and El-Demerdash, 2006). The delicate balance between the production and catabolism of oxidants is critical for maintaining biological functions (Sridevi et al., 1998). Srivastava et al. (1983) have reported an increase in thiobarbituric acid-reactive substances (TBARS) at certain critical levels of glutathione (GSH) depletion. Acrylamide is oxidized to glycidamide, a reactive epoxide, and undergoes a conjugation reaction with GSH (Dybing and Sanner, 2003). Additionally, acrylamide interacts with other vital cellular nucleophiles containing –SH, –NH$_2$ or –OH groups and forms glutathione S-conjugates, which is the initial step in the biotransformation of electrophiles to mercapturic acids (Awad et al., 1998). Furthermore, glutathione is an important reducing agent and cellular antioxidant in mammalian cells (Tong et al., 2004).

The neurotoxicity of acrylamide has been extensively studied in mammals (i.e., rats, mice, monkeys, guinea pigs, dogs and cats) with daily administration (0.5-50 mg/kg/day) (LoPachin and Lehning, 1994; LoPachin et al., 2002, 2003). The overt signs of acrylamide-induced neurotoxicity are consistent across species. In well described rodent models, acrylamide exposure at 15-50 mg/kg/day produces several neurological deficits, including hind-limb foot splay, decreased fore- and hind-limb grip strength, ataxia and skeletal muscle weakness (Burek et al., 1980; Moser et al., 1992; Shell et al., 1992; Crofton et al., 1996; LoPachin et al., 2002).

Previous studies using rats have suggested that axon degeneration might not be a primary effect of acrylamide exposure (LoPachin et al., 2000; Lehning et al., 2003). Specifically, peripheral nerve (sciatic, tibial and sural nerves) degeneration was restricted to low-dose/long-term acrylamide exposures (21 mg/kg/day) (Lehning et al., 2002). A recent silver stain study of rat cerebellum revealed that both acrylamide doses (21 and 50 mg/kg/day) produced progressive degeneration of Purkinje cell axons

(Lehning et al., 2003). Moreover, acrylamide exposure resulted in central-peripheral neuropathy in humans and in laboratory animals, including rats and monkeys (LoPachin, 2004; Seale et al., 2012). This study aimed to determine the developmental effects on neonatal rat pups (weight, external features, cerebrum and oxidative stress) after oral maternal exposure to acrylamide monomers in albino rats during pregnancy and lactation.

Materials and Methods

Chemicals: Acrylamide (99% pure) and other chemicals were purchased from Sigma Chemical Company (St Louis, MO, USA). All other chemicals used were of analytical grade.

Animal dosing schedule: Sixty albino rats (*Rattus norvegicus)* were used in this study. Forty-five mature virgin females and 15 mature males weighing 140-150 g were purchased from the Organization for Vaccine and Biological Preparations (Helwan Laboratory Farms, Egypt). Animals were marked, housed 4 per cage and fed a standard rodent pellet diet that was manufactured by the Egyptian Company for Oil and Soap (Cairo, Egypt). Tap water was given *ad libitum.* A vaginal smear from each virgin female was examined daily to determine their estrous cycle. The vaginal smear of estrous females contains cornified cells. Mating was performed by housing 2 pro-estrous females with one male overnight. The presence of sperm in the vaginal smear was identified as D0 of gestation. Acrylamide was dissolved in distilled water and administered orally to non-anesthetized pregnant rats by gastric intubation at a dose of 10 mg/kg/day. This chronic dose was used because higher doses will reduce the reproductive activity of the dams and cause paralysis (Tyl *et al.*, 2000).

The dams were separated into the following three groups as follows:

Group A: Pregnant dams were given saline (*control*).

Group B: Pregnant dams were administered acrylamide from D7 of gestation until birth (*prenatal* exposure).

Group C: Pregnant dams were administered acrylamide from D7 of gestation until D28 after birth (*perinatal* exposure).

Postnatal investigations: The neonatal pups were monitored daily, and the following notes were recorded for each group as follows:

1. The weights of six neonatal pups from each group were recorded daily.
2. The time of fur appearance.
3. The time of ear opening.
4. The time of eye opening.

Biochemical assays

Pups from each group were sacrificed by decapitation at D7, D14, D21 and D28. The cerebra were dissected, and 0.25 g of tissue from each pup was homogenized in 3 ml of cold saline. Each homogenate was centrifuged at 10,000 ×g for 10 min at 4 $^\circ$C, and 0.5 ml of the clear supernatant was collected in a microfuge tube and stored at -40 $^\circ$C.

Lipid peroxidation (TBARS)

Lipid peroxidation was determined by assaying for TBARS according to the method of Preuss et al. (1998). Briefly, 1.0 ml of supernatant was precipitated with 2 ml of 7.5% trichloroacetic acid and centrifuged at 1,000 ×g for 10 min. The clear supernatant was mixed with 1 ml of 0.70% thiobarbituric acid and incubated at 80 $^\circ$C, and the absorbance was then measured at 532 nm. Tetramethoxypropane was used as a standard.

GSH assay

The concentration of glutathione was determined according to the method described by Beutler *et al*. (1963) with some modifications. Briefly, 0.20 ml of tissue supernatant was mixed with 1.5 ml of a precipitating solution containing 1.67% glacial metaphosphoric acid, 0.20% Na-EDTA and 30% NaCl. The mixture was incubated for 5 min at room temperature and centrifuged at 1,000 ×g for 5 min. One milliliter of the clear supernatant was mixed with 4 ml of 0.30 M Na_2HPO_4 and 0.50 ml of DTNB reagent (40 mg of 5,5'dithiobis-(2-nitrobenzoic acid) dissolved in 1% sodium citrate). Similarly, a blank was prepared with 0.20 ml of water instead of the cerebrum supernatant. The absorbance was measured at 412 nm with a spectrophotometer.

Total thiol determination

Total thiol concentration was determined according to the method of Koster *et al.* (1986). Briefly, 50 µl of the supernatant and 0.75 ml of 0.1 M phosphate buffer (*p*H 7.4) was mixed with 0.20 ml of Ellman's reagent (2 mM 5,5'dithiobis-(2-nitrobenzoic acid)) and incubated for 5 min at 37 $^\circ$C. A blank was prepared with 50 µl of water instead of the cerebrum supernatant. The absorbance was measured at 412 nm with a spectrophotometer.

Superoxide dismutase (SOD) assay

SOD activity was assayed using the method of Marklund and Marklund (1974). Briefly, 1.0 ml of supernatant was mixed with 0.10 ml of Tris/EDTA buffer (pH 8.0) and 0.05 ml of freshly prepared 10 mM pyrogallol. A control was prepared by adding 1.0 ml of water instead of the cerebrum extract. The difference in the absorbance at 430 nm at zero min and after 10 min was used to calculate the enzyme activity.

Peroxidase activity

Peroxidase activity was determined using the method of Kar and Mishra (1976). Briefly, 1.0 ml of supernatant was mixed with 3.0 ml of 0.01 M phosphate-buffered saline (*p*H 6.8), 315 µl of 2% pyrogallol and 154 µl H_2O_2 and was incubated for 15

min at 25 $^{\circ}$C. The reaction was stopped by adding 0.50 ml of 5% H_2SO_4, and the absorbance was measured at 420 nm. Peroxidase activity was expressed as the amount of purpurogallin formed per absorbance unit.

Light microscopy

Cerebral segments (5 mm) at D7, D14, D21 and D28 were fixed in 20% buffered formalin (*pH* 7.4) for 24 hour. The tissue was dehydrated in ethyl alcohol followed by two xylene washes. The tissue was impregnated with paraffin wax and then embedded in paraffin wax. Sections (4-5 µm) were cut, de-waxed, hydrated and stained with Mayer's hemalum solution for 3 min. Next, the sections were stained in eosin for one min, washed in tap water and dehydrated in ethanol as described above. Hematoxylin and eosin-stained sections were prepared according to the method of Mallory (1988). Toluidine blue stain for Nissl granules and protein was used according to Carleton *et al*. (1967). The Feulgen method was used for DNA staining (Feulgen and Rossenbeck, 1924).

Statistical analysis

The Statistical Package for the Social Sciences (SPSS for Windows, version 11.0; SPSS Inc., Chicago, IL) was used for the statistical analyses. Comparative analyses were conducted using the general linear models procedure (SPSS, Inc.). Additionally, the data were analyzed using one-way and two-way analysis of variance (ANOVA) followed by LSD computations to compare various groups with each other. The results are expressed as the means S.D. Differences were considered significant at P<0.05 and highly significant at P<0.01 (Rao and Blane, 1995).

Results

1. General developmental observations

The neonatal pups in group B were exposed to acrylamide prenatally, while the neonatal pups in group C were exposed to acrylamide perinatally. Signs of acrylamide toxicity, including ataxia, splayed hind limbs, weakness of hind-limb muscles and paralysis causing alterations in maternal behavior, were observed in the treated dams after birth; thus, the neonatal pups suffered from poor lactation and malnutrition, especially in group C. At birth, all pups were hairless. The times of fur appearance and ear and eye opening were delayed in groups B and C (Table 1). The mean pup weights in all experimental groups varied between D1 and D28 (Table 2).

2. Oxidative stress

2.1. TBARS

Data of the toxic effects of prenatal and perinatal acrylamide exposure on the cerebral lipid peroxidation content of neonatal rat pups are presented in Table 3. In group A, lipid peroxidation decreased with age. Acrylamide exposure induced a significant increase in lipid peroxidation at all time points, with a maximum

increase at D7 in group C. Table 3 illustrates the significant difference in lipid peroxidation between control and treated neonatal pups.

2.2 GSH content

The exposed pups exhibited a significant decrease in cerebral glutathione content compared with control pups, especially in the perinatally exposed group. In groups A and C, GSH contents decreased with age, while there were some fluctuations in group B. Table 3 presents the differences in cerebral GSH content due to prenatal and perinatal acrylamide exposures.

2.3 Total thiol content

Table 3 indicates that cerebral total thiol levels increased significantly with age in the control group and fluctuated in the treated groups. The total cerebral thiol contents were reduced in the prenatal and perinatal exposure groups. These reductions were highly significant (P 0.001) in group C.

2.4 Peroxidase activity

Acrylamide-exposed neonatal pups exhibited a highly significant (P 0.001) decrease of cerebral peroxidase activity (Table 4). The highest reduction in cerebral peroxidase activity was measured at the end of the experiment in group C. Peroxidase activity varied slightly with age throughout the experiment.

2.5 SOD activity

SOD activity was significantly (P 0.001) decreased in the cerebra of the exposed groups compared to the control groups at all time points (Table 4). This decrease in activity was more pronounced over time in group C. In unexposed and exposed neonatal pups, cerebral SOD activity changed with age.

3. Histological study of the cerebral cortex

3.1 Hematoxylin-eosin stain

In control and treated neonatal pups at D7, the border between the cerebral cortex layers was undetectable. The outer most layer of the gray matter lies just below the pia mater, a delicate connective tissue, and is the outermost molecular layer that is defined at this age because it does not contain neurons (Figs. 1a, b and c). Additionally, normal cerebral cortex cells were large, and their apical dendrites were perpendicular to the pial surface, while in the treated groups, cells were small and undifferentiated (Figs. 1d, e and f). At D14, the normal pyramidal cells exhibited their general characteristic shape. The nuclei of these cells were rounded, large and centrally located (Figs. 1g and j). At D21, the outer molecular layer was sharply defined (Figs. 2a and d). The normal cells of the cerebral cortex at D28 exhibited a spherical or pyramidal perikaryon with large nuclei; additionally, the neurons were arranged in a regular pattern (Figs. 2g and j). The cerebral neurons appeared more developed toward the white matter (Figs. 2a and g).

Pathological cases were observed in sections from the neonatal pups in the treated groups. In treated group B, pyknosis was observed at D14, D21 and D28 (Figs. 1k, 2e and k). In treated group C, high levels of neurocyte chromatolysis were observed (Figs. 1l, 2f and l).

3.2 Toluidine blue stain

Nissl granules of the normal cerebral cortex cells appeared as compact bodies in the form of flakes and granules. These granules were arranged around the nucleus and at the proximal parts of dendrites. The intensity of Nissl granule staining in the cytoplasm increased with age from D7 to D28 (Figs. 3a, d, g and j).

At D7, the cytoplasms of the pyramidal neurons in the control group were distinctly stained (Fig. 3a) but stained faintly in groups B and C (Figs. 3b and c). Similar results were observed at D14 in all groups (Figs. 3d, e and f). At D21, the normal pyramidal cells were moderately stained in group B, which reflected the increase in Nissl granule content in the pyramidal cells, but were stained faintly in group C (Figs. 3g, h and i). The results from D28 were similar to those observed at D21 (Figs. 3j, k and l).

3.3 Feulgen stain

The Feulgen reaction was used to visualize the DNA content in cerebral cortex cells. DNA-containing particles of normal cerebral cells were strongly stained red to pink (Figs. 4a, d, g and j). Furthermore, the color intensity in the cells from the control group increased with age. The staining intensity of the nuclei from groups B and C was markedly decreased, indicating the loss of DNA during chromatolysis (Figs. 4b, c, e, f, h, i, k and l).

Discussion

This study was designed to examine the effect of acrylamide on body weight, cerebral development and the appearance of some external features in neonatal rat pups after different maternal acrylamide exposure conditions. The effects of this low-dose acrylamide exposure were recorded in several sections of the cerebral cortex at different postnatal time points.

Acrylamide and its metabolite, glycidamide, pass readily through the placenta due to their solubility in water (Sorgel *et al*., 2002) and are distributed in many fetal tissues during gestation (Marlowe *et al*. 1986 and Sumner *et al*., 2001). In addition, acrylamide leads to poor lactation due to changes in maternal behaviors (Frieda and William, 1999 and Shaheed *et al*., 2006). Therefore, the neonatal pups from groups B and C suffered from acrylamide exposure and malnutrition.

Pups in group B were prenatally exposed to acrylamide. In addition, these pups suffered from postnatal malnutrition because maternal acrylamide exposure during gestation leads to poor maternal behaviors (Shaheed *et al*., 2006). In group C, the neonatal pups were exposed to acrylamide during gestation and lactation, which also led to malnutrition.

In control neonatal pups, fur appeared at D9. The appearance of fur was delayed in the treated groups. Gold and Schaumberg (2000) reported that acrylamide exposure causes growth retardation. In control neonatal pups, ear opening was detected at D12-13. Smart *et al*. (1971) detected similar results in neonatal rat pups. In the treated groups, ear opening was delayed until D15. This delay indicates that acrylamide exposure impairs organogenesis, as mentioned by Marlowe *et al*. (1986). Additionally, these results are in agreement with the results reported by Garey *et al*. (2005). Eye opening occurred at D14-15 in group A, which is in agreement with data from Bolles and Woods (1964); however, eye opening was detected at D16-17 in groups B and C. This delay in the treated groups is in agreement with Sumner *et al*. (2001), who reported that acrylamide causes developmental alterations.

The neonatal pups of the treated dams had reduced body weights. Prenatal weight reduction results mainly from intrauterine acrylamide exposure that leads to growth deficiency in the developing fetus (Tyl *et al*., 2000). In addition, body weight was the most sensitive indicator of developmental toxicity in neonatal pups (Wise *et al*., 1995). In this study, the effects of acrylamide on the embryos were intrauterine because fetuses do not have the enzymes required for acrylamide metabolism once it has entered the blood supply (Adlard and Dobbing, 1971). In the treated groups, acrylamide affects mammary gland function through prolactin reduction, which impairs lactation (Uphouse *et al*., 1982). Therefore, malnutrition and subsequent reductions in body weight were observed in treated neonatal pups. Frieda and William (1999) stated that postnatal weight reduction in treated neonatal pups occurs because of altered maternal behaviors and reduced lactation caused by the acrylamide exposure.

Maternal acrylamide exposure during gestation and lactation increased oxidative stress and suppressed the antioxidant defense system in the cerebra of neonatal rat pups in this study. The lipid peroxidation level was significantly increased, while GSH and total thiol levels were significantly depleted. Moreover, the activities of the antioxidant enzymes SOD and peroxidase were reduced in the treated groups. Group C exhibited the most pronounced effects due to perinatal acrylamide exposure. In the control group, biochemical parameters and oxidative stress changed in the neonatal pups with age due to maturation and tissue differentiation. Yousef and El-Demerdash (2006) indicated that rats receiving oral acrylamide exhibited significant elevations in lipid peroxidation. Bhadauria *et al*. (2002) and Uličná *et al*. (2003)

observed that acrylamide exposure increases hepatic malondialdehyde levels and reduced GSH levels. Srivastava *et al.* (1983) suggested that the increase in lipid peroxidation (TBARS) results from glutathione depletion to certain critical levels.

The increase in TBARS observed in this study is in agreement with the decrease in GSH concentration in the cerebra of acrylamide-treated neonatal pups. GSH is a powerful reducing agent that can interrupt free-radical lipid peroxidation. Furthermore, lipid peroxidation of polyunsaturated lipids has been implicated in a variety of disease states (Ghosh *et al.,* 1994). The delicate balance between the production and catabolism of oxidants is critical for the maintenance of biological function (Allam et al., 2010).

Glutathione is an essential compound for maintaining cell integrity because of its reducing properties and its participation in cell metabolism (Conklin, 2000). Alterations in the ratio of GSH and oxidized glutathione have been used as indicators of oxidative stress and diseases in humans and laboratory animals (Gohil *et al.,* 1988). In states of oxidative stress, GSH is converted into the oxidized form, GSSG, and is then depleted, which leads to lipid peroxidation. Therefore, GSH is an important marker for the evaluation of oxidative stress (Recknagel *et al.*, 1991). To prevent lipid peroxidation, it is crucial to maintain GSH levels. GSSG is reduced to GSH by glutathione reductase (GR), which is NADPH-dependent. However, free radicals and lipid peroxides, formed by acrylamide, interact with the sulfhydryl (SH) group present at the active site of the GR, leading to its reduction. The reduction of GR inhibits enzymatic activity, preventing the reduction of GSSG, thus decreasing GSH (Recknagel *et al.*, 1991; Yousef and El-Demerdash, 2006**)**. Furthermore, GST catalyzes the conjugation of glutathione thiol functional groups to electrophilic xenobiotics to increase solubility. The xenobiotic-GSH conjugate is then eliminated or converted to mercapturic acid (Rao *et al.*, 2006). Acrylamide reacts with glutathione by interacting with vital cellular nucleophiles containing –SH, –NH$_2$ or –OH groups and forms glutathione S-conjugates, the initial step in the biotransformation of electrophiles into mercapturic acids (Awad *et al.*, 1998). A decrease in tissue GSH levels with higher acrylamide exposures could be caused by the increased formation of S-conjugates between acrylamide and GSH. Thiol groups are required for the activity of many biologically important proteins. Additionally, thiol groups are important reducing agents and cellular antioxidants (Yousef and El-

Demerdash, 2006). Meng *et al.* (2001) found that 0–1 M acrylamide exposure significantly depleted protein thiols, which is in agreement with the results of this study.

The antioxidant enzymes SOD, catalase and peroxidases constitute a mutually supportive team for the defense against reactive oxygen species (Tabatabaie and Floyd, 1994 and Bandhopadhay *et al.*, 1999). The decreases in SOD and peroxidase activities in the acrylamide-exposed neonatal pups may be caused by increased lipid peroxidation or the inactivation of the enzymes by malondialdehyde cross-linking. These effects will result in the increased accumulation of superoxide and hydrogen peroxide radicals that could further stimulate lipid peroxidation (Rister and Bachner, 1976 and Rajesh and Latha, 2004). The peroxidase assayed in this study, which uses pyrogallol as a substrate, may be myeloperoxidase or eosinophil peroxidase (heme peroxidase) rather than glutathione peroxidase, which is highly specific for glutathione and cannot oxidize any other substrates (Shigeoka *et al.*, 1991).

Based on these data, it is important to note that enhanced lipid peroxidation and the deterioration of the antioxidant defense system resulting from acrylamide exposure may play significant roles in the pathogenesis and deleterious histological effects observed in the cerebra of neonatal pups. The normal pyramidal neurons exhibited a pyramidal perikaryon with apical dendrites projecting toward the pial surface; similar observations have been documented in humans (Zhang, 1999), monkeys (Kogan *et al.*, 2000), rabbits and guinea pigs (Dalia, 2002). In agreement with the gradient migration theory of neurons, in this study, the cerebral neurons of rat neonatal pups appeared more gradually developed toward the white matter. Therefore, these observations follow the inside-out gradient theory of neuron migration. An explanation for the origin of the inside-out gradient has been previously detailed by Marin-Padilla (1998) and Dalia (2002).

In this study, the most striking features of acrylamide toxicity in the cerebral cortex were pyknosis and neurocyte chromatolysis, which were detected at all investigated stages. The severity of neurocyte chromatolysis increased with age in group C. As stated by He *et al.* (1989), Deng *et al.* (1993) and LoPachin (2004), these pathological cases reflect a CNS neuropathy caused by acrylamide exposure. This damage may result from the metabolic and biochemical alterations caused by acrylamide and its metabolites (Seale et al., 2012).
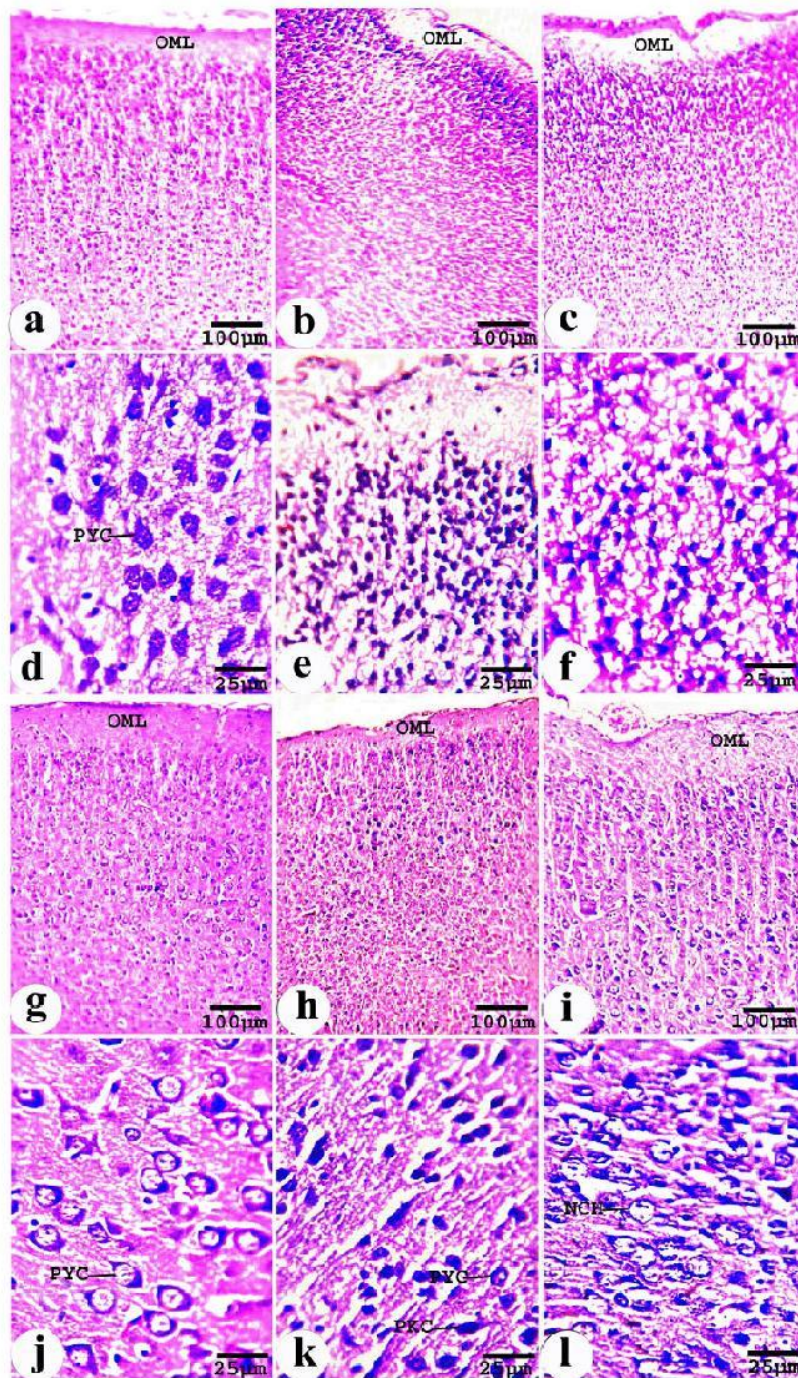
Fig. 1. Sagittal sections of the cerebral cortex depicting the outer molecular layer (OML), pyramidal cell distribution (PYC), neurocyte chromatolysis (NCH) and pyknosis (PKC) in the following groups: (**a**, **d**) control group at D7, (**b**, **e**) group B at D7, (**c**, **f**) group C at D7, (**g**, **j**) control group at D14, (**h**, **k**) group B at D14 and (**i**, **l**) group C at D14. Scale bar = 100 µm in a, b, c, g, h and i and 25 µm in d, e, f, j, k and l. (**H and E**)
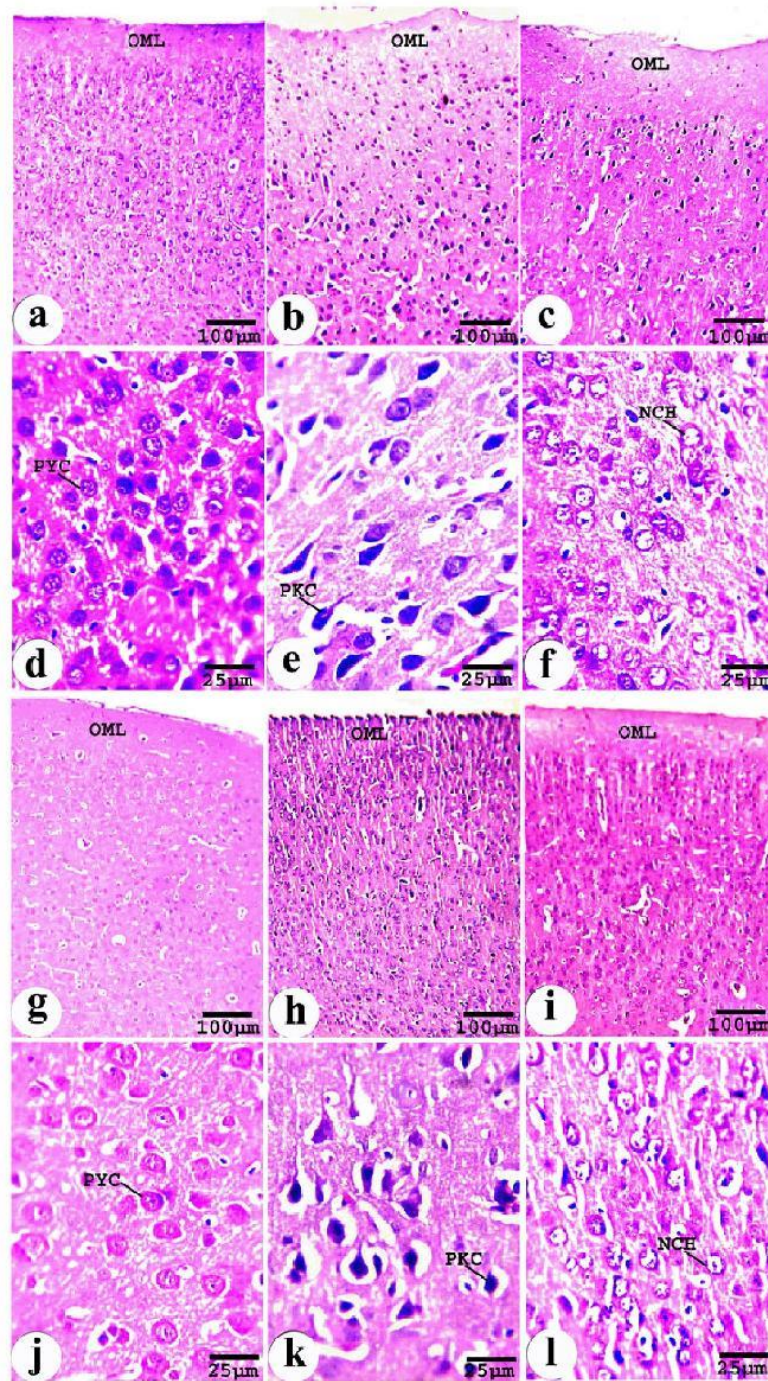
Fig. 2. Sagittal sections of cerebral cortices depicting neurocyte chromatolysis (NCH), the outer molecular layer (OML), pyramidal cell distribution (PYC) and pyknosis (PKC) in the following groups: (**a**, **d**) control group at D21, (**b**, **e**) group B at D21, (**c**, **f**) group C at D21, (**g**, **j**) control group at D28, (**h**, **k**) group B at D28 and (**i**, **l**) group C at D28. Scale bar = 100 µm in a, b, c, g, h and i and 25 µm in d, e, f, j, k and l. (**H and E**)
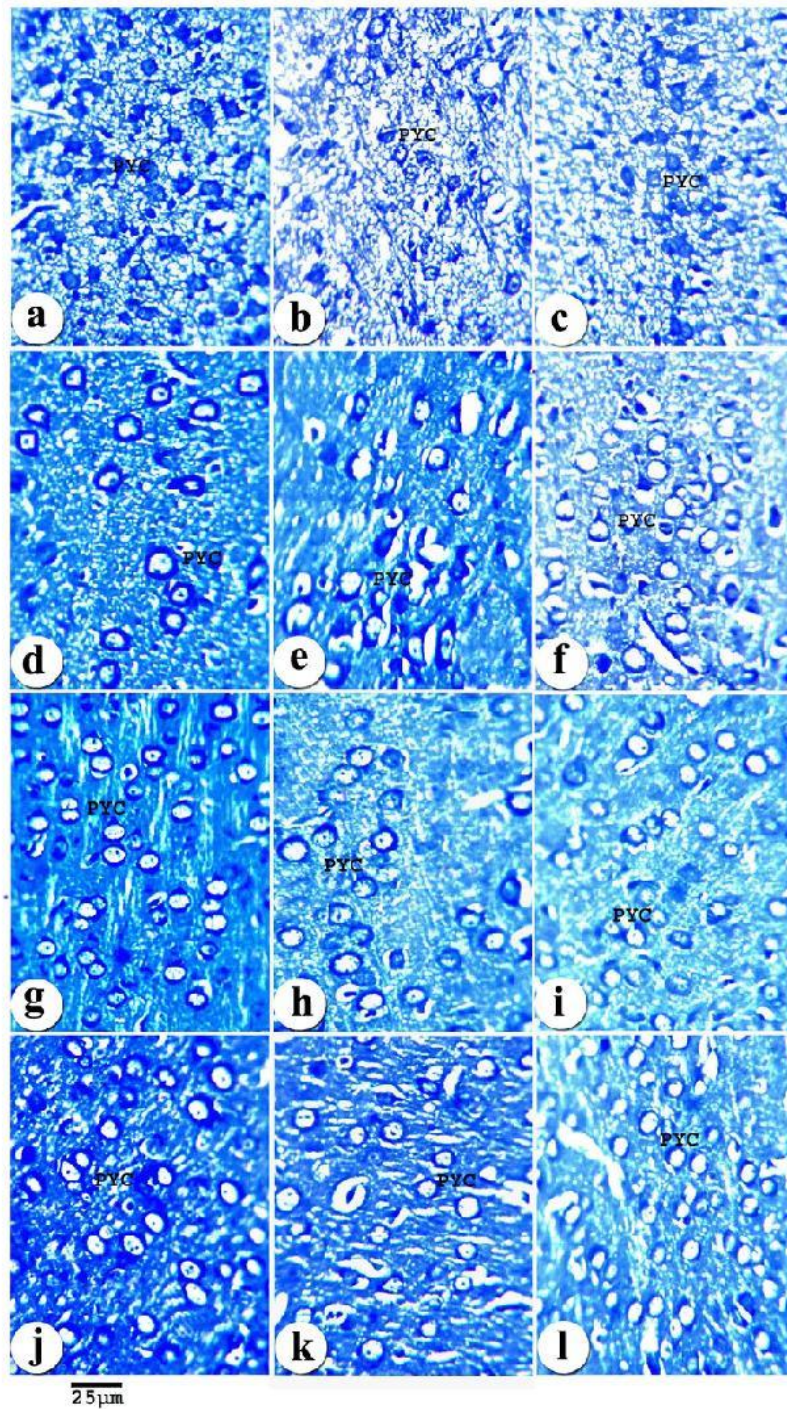
Fig. 3. Sagittal sections of cerebral cortices depicting the distribution of Nissl granules in pyramidal cells (PYC) of the following groups: (**a**) control group at D7, (**b**) group B at D7, (**c**) group C at D7, (**d**) control group at D14, (**e**) group B at D14, (**f**) group C at D14, (**g**) control group at D21, (**h**) group B at D21, (**i**) group C at D21, (**j**) control group at D28, (**k**) group B at D28 and (**l**) group C at D28. Scale bar = 25 μm. (**Toluidine blue stain**)
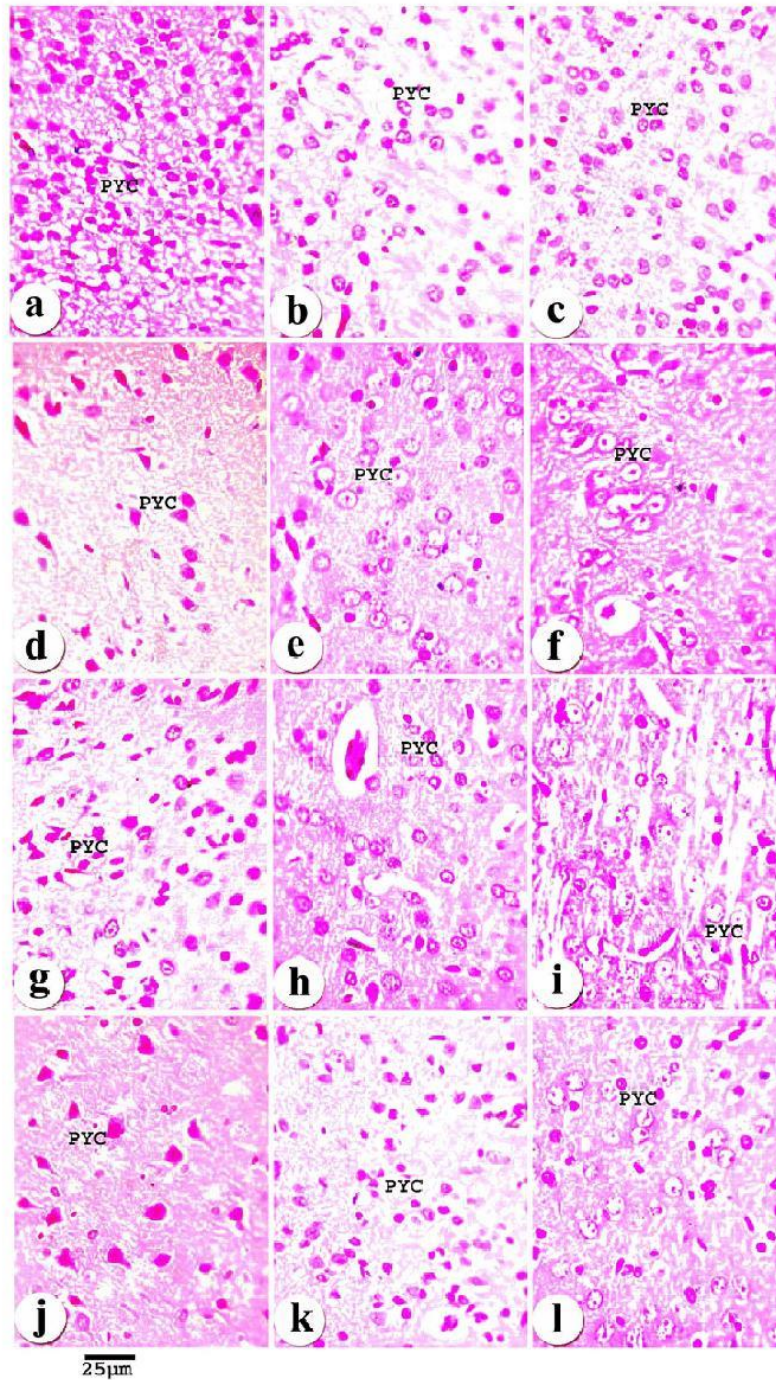
Fig. 4: Sagittal sections of cerebral cortices depicting DNA in the nuclei of pyramidal cells (PYC) of the following groups: (**a**) control group at D7, (**b**) group B at D7, (**c**) group C at D7, (**d**) control group at D14, (**e**) group B at D14, (**f**) group C at D14, (**g**) control group at D21, (**h**) group B at D21, (**i**) group C at D21, (**j**) control at D28, (**k**) group B at D28 and (**l**) group C at D28. Scale bar = 25 μm. (**Feulgen staining technique**)

Table 1 External features appearance in rat newborns.

Features/Groups	A	B	C
Fur appearing	D9	D11-12	D12-13
Ear opening	D12-13	D15	D15
Eye opening	D14-15	D16-17	D16-17

Table 2 Changes of body weights in rat newborns.
Data are expressed as a mean ± S.E. (N =6)
Values significantly compared to the control newborns; p* ≤0.05, p** ≤0.01and p*** ≤0.001.

D/ Groups	A	B	C
1	6.31±0.12	5.08±0.13***	3.88±0.11***
2	7.4±0.26	5.15±0.08***	4.47±0.50**
3	8.33±0.19	5.53±0.16***	5.27±0.38**
4	9.15±0.15	5.57±0.11***	5.83±0.53***
5	9.58±0.28	5.8±0.13***	5.48±0.29***
6	10.65±0.23	6±0.21***	6.23±0.40***
7	12.13±0.16	6.83±0.27***	6.18±0.27***
8	13.57±0.1	6.85±0.41***	6.75±0.31***
9	14.27±0.13	9.23±0.68***	7.13±0.38***
10	16.1±0.15	10.9±0.336***	7.9±0.30***
11	17.23±0.13	10.47±0.63***	9.33±0.77***
12	17.33±0.07	10.77±0.41***	9.85±0.80***
13	18.25±0.09	12.27±0.81***	9.27±0.65***
14	19.35±0.15	11.58±0.72***	9.33±0.67***
15	20.35±0.08	13.28±0.68***	10.72±0.60***
16	21.60±0.15	15.38±0.42***	10.39±0.34***
17	23.67±0.36	16.93±0.76**	12.93±0.61***
18	23.97±0.36	17.36±0.78***	11.3±0.56***
19	25.22±0.51	19.73±0.40***	11.63±0.60***
20	25.8±0.64	20.68±0.69***	12.47±0.70***
21	27.75±0.60	20.9±0.38***	14.18±0.50***
22	28.47±0.52	21.2±0.51***	16.48±0.47***
23	31.42±0.45	22.85±0.71***	20.12±0.95***
24	34.52±0.35	23.68±0.99***	20.97±0.87***
25	36.07±0.37	23.55±0.77***	21.55±1.13***
26	38.45±0.57	24.65±0.99***	22.40±1.12***
27	39.65±0.62	25.87±77***	23.25±0.64***
28	43.17±0.99	26.62±0.62***	24.21±1.11***

Table 3 Effect of acrylamide administration on the development of cerebral TBARS, GSH and total thiol contents in rat newborns.
Data are expressed as mean S.D. (N = 6)
Means which share the same superscript are not significantly different; significance level = 0.05

Parameter	Group /Time	D7	D14	D21	D28
TBARS (nmol/100mg)	Normal	24.67 3.10[e]	19.37 1.60[f]	19.05 1.20[f]	18.74 1.33[f]
	Group B (prenatal)	27.07 1.96[cd]	27.33 2.22[c]	27.56 2.23[c]	25.45 2.67[cd]
	Group C (perinatally)	40.10 3.05[a]	31.47 2.81[b]	27.83 1.01[c]	26.29 2.14[cd]
GSH (nmol/gm)	Normal	57.51 6.06[a]	54.31 2.86[ab]	51.12 2.86[b]	50.59 2.41[b]
	Group B (prenatal)	36.21 3.30[c]	34.07 5.22[c]	38.27 5.981[c]	34.61 3.14[c]
	Group C (perinatally)	28.22 3.14[d]	27.16 1.74[d]	23.96 3.91[d]	23.64 4.33[d]
Total Thiol (mol/gm)	Normal	1.67 0.07[c]	1.87 0.14[b]	2.24 0.09[a]	2.35 0.14[a]
	Group B (prenatal)	1.00 0.23[de]	0.99 0.13[de]	1.15 0.18[d]	1.70 0.18[bc]
	Group C (perinatally)	0.94 0.19[ef]	0.81 0.11[f]	0.84 0.12[ef]	0.89 0.16[ef]

Table 4 Effect of acrylamide administration on the development of cerebral peroxidase and SOD activities in rat newborns.

Data are expressed as mean S.D. (N = 6)

Means which share the same superscript are not significantly different; significance level = 0.05.

Parameter	Group/Time	D7	D14	D21	D28
Peroxidase (U/gm)	Normal	44.61 1.42[a]	44.68 1.30[a]	44.13 1.341[a]	43.03 2.00[a]
	Group B (prenatal)	37.85 0.87[b]	35.08 0.72[cd]	38.87 1.59[b]	38.49 1.28[b]
	Group C (perinatally)	34.71 1.43[cd]	33.55 2.58[d]	35.75 1.15[c]	35.86 1.55[c]
SOD (U/gm)	Normal	6.34 1.19[b]	6.72 1.53[b]	10.70 2.08[a]	9.48 2.16[a]
	Group B (prenatal)	3.22 0.86[de]	3.68 0.48[de]	4.59 0.63[c]	4.00 0.53[de]
	Group C (perinatally)	3.40 0.44[de]	3.02 0.42[e]	4.51 0.65[cd]	3.75 0.38[de]

References

1. Adlard B, Dobbing J. Vulnerability of developing brain. III. Development of four enzymes in the brains of normal and undernourished rats. Brain Res 1971; 28: 97-107.
2. Allam A, El-Ghareeb A, Abdul-Hamid M, Baikry A, Sabri M. Prenatal and perinatal acrylamide disrupts the development of cerebellum in rat: Biochemical and morphological studies. Toxicol Ind Health 2011; 27(4): 291-306.
3. Allam A, El-Ghareeb AW, Abdul-Hamid M, Bakery AE, Gad M, Sabri M. Effect of prenatal and perinatal acrylamide on the biochemical and morphological changes in liver of developing albino rat. Arch Toxicol 2010; 84 (2): 129-41.
4. Bolles RC, Woods PJ. The ontogeny of behavior in the albino rat. Anim. Behav 1964; 12: 427-441.
5. Cabana T, Cassidy G, Pflieger JF, Baron G. The ontogenic development of sensorimotor reflexes and spontaneous locomotion in the Mongolian gerbil (*Meriones unguicutas*). Brain Res Bull 1993; 30: 291-301.
6. Carleton H, Drury R, Willington E, Conergon H. Cited from Carleton. Histological Techniques. 4th Ed. Oxford Univ. Press No. 4, Toronto1967.
7. Cavanagh JB, Gysbers MF. Ultrastructureal features of the Purkinje cell damage caused by acrylamide in the rat: a new phenomenon in cellular neuropathology. Neurocytology 1983; 12: 413-437.
8. Crofton KM, Padilla S, Tilson HA, Anthony DC, Raymer JH, MacPhail RC. The impact of dose rate on the neurotoxicity of acrylamide: the interaction of administered dose, target tissue concentrations, tissue damage, & functional effects. Toxicol Appl Pharmacol 1996; 139: 163-76.
9. Dalia MS. Comparative Studies on The Ontogeny of Sensorimotor Reflexes and Locomotive Activity in Small Mammals and Their Applications on Infants. Ph. D. Thesis, Fac. of Science, Mansour Univ. Egypt 2002.
10. Feulgen R, Rossenbeck H. Mikroskopisch Chemischer Nach weis einen Nucleinsaure von Typus der Thymonucleinsaure und de darauf berhende elective Farbung von Zelkernen in microskopischen preparaten. Zeitschrift Physiol Chem 1924; 135: 203.
11. Frieda SG, William PR. Effects of lactational administration of acrylamide on rat dams and offspring. Rep. Toxicol 1999; 13: 511-520.
12. Garey J, Sherry AF, Merle GP. Developmental and behavioral effects of acrylamide in Fischer 344 rats. Neurotoxicol and Teratol 2005; 27(4): 553-563.
13. Gold BG, Schaumberg HH, Spencer PS, Schaumberg HH, Ludolph A. Experimental and Clinical Neurotoxicol, 2nd Ed., Oxford University Press, pp124–132, New York 2000.
14. Klaunig JE, Kamendulis LM. Mechanism of acrylamide induced rodent carcinogensis. Adv Exp Med Biol 2005; 561: 49-62.
15. Ko MH, Chen WP, Linshiau SY, Hsieh ST. Age-dependent acrylamide neurotoxicity in mice: morphology, physiology and function. Exp Neurol 1999; 158(1): 37-46.
16. Lehning EJ, Balaban CD, Ross JF, LoPachin RM. Acrylamide neuropathy: III- Spatiotemporal charcteristics of nerve cell damage in forebrain. Neurotoxicology 2003; 24: 125-136.
17. Lehning EJ, Balaban CD, Ross JF, Reid MA, LoPachin RM. Acrylamide neuropathy. I- Spatiotemporal characteristics of nerve cell damage in rat cerebellum. Neurotoxicology 2002: 23; 397-416.
18. LoPachin RM. The changing view of acrylamide neurotoxicity. Neurotoxicology 2004; 25: 617-630.
19. LoPachin RM, Lehning EJ. The relevance of axonal swellings and atrophy to gamma diketone neurotoxicity a forum position paper. Neurotoxicology 1997; 18: 7-22.
20. LoPachin RM, Lehning EJ, Opanashuk LA, Jortner BS. Rate of neurotoxicant exposure determines morphologic manifestations of distal axonopathy. Toxicol Appl Pharmacol 2000; 167: 75–86.

21. LoPachin RM, Schwarcz AI, Gaughan CL, Mansukhani S, Das S. *In vivo* and *in vitro* effects of acrylamide on synaptosomal neurotransmitter uptake and release. Neurotoxicology 2004; 25: 349-363.

22. Ma Y, Shi J, Zheng M, Liu J, Tian S, He X, Zhang D, Li G, Zhu J. Toxicological effects of acrylamide on the reproductive system of weaning male rats. Toxicol Ind Health 2011; 27(7): 617–27.

23. Maier A, Kohrman-Vincent M, Hertzberg R, Allen B, Haber LT, Dourson M. Critical review of dose-response options for F344 rat mammary tumors for acrylamide - Additional insights based on mode of action. Food Chem Toxicol 2012; 50(5):1763-75.

24. Mallory FB. Pathological Techénique. W. B. Saunders, Philadelphia 1988.

25. Marlowe C, Clark MJ, Mast RW. The distribution of (14C) acrylamide in male and pregnant Swiss Webster mice by whole body autoradiography. Toxicol Appl Pharmacol 1986; 86: 457-465.

26. Rajaoftra N, Sandillon F, Geffard M, Privat A. Pre-and postnatal ontogeny of serotonergic projections to the rat spinal cord. J Neurons Res 1989; 22: 305-321.

27. Seale SM, Feng Q, Agarwal AK, El-Alfy AT. Neurobehavioral and transcriptional effects of acrylamide in juvenile rats. Pharmacol Biochem Behav 2012; 101(1): 77-84.

28. Sega GA, Valdivia RP, Tancongco CP, Brimer P. Acrylamide binding to the DNA and protamine of spermiogenic stages in the mouse and its relationship to genetic damage. Mutat Res 1989; 216: 221-230.

29. Shaheed IB, Kawkab AA, Makhlouf MM. Toxicicological and pathological studies on acrylamide neurotoxicity in albino rats. Egypt J Comp Pathol Clin Pathol 2006; 19: 63-82.

30. Smart JL, Dobbing J. Vulnerability of developing brain. II. Effects of early nutritional deprivation on reflex ontogeny and development of behaviour in the rat. Brain Res 1971; 28: 85-95.

31. Sorgel F, Weissenbacher R, Kinzig-Schippers M, Hofmann A, Illauer M, Skott A, Landersdorfer C. Acrylamide increased concen-trations in homemade food and first evidence of its variable absorption from food, variable metabolism and placental and breast milk transfer in humans. Chemotherapy 2002; 48: 267-274.

32. Spencer PS, Schaumburg HH. Ultrastructural studies of the dying-back process. III- The evolution of experimental peripheral giant axonal degeneration. J Neuropathol Exp Neurol 1977a; 36: 276-99.

33. Spencer PS, Schaumburg HH. Ultrastructural studies of the dying-back process. IV- Differential vulnerability of PNS and CNS fibers in experimental central-peripheral distal axonopathy. J Neuropathol Exp Neurol 1977b; 36: 300-20.

34. Sridevi B, Reddy KV, Reddy SN. Effect of trivalent and hexavalent chromium on antioxidant enzyme activities and lipid peroxidation in a freshwater field crab, *Barytelphusa guerini*. Bull. Environ. Contam Toxicol 1998; 61: 384-390.

35. Sterman AB. Acrylamide induce early morphologic reorganization of the neuronal cell body. Neurology 1982; 32: 1023-1026.

36. Stevens A, Lowe J. Human Histology; 2nd Ed., Grafos SA, Arte Sobre Papel, Spain 1997.

37. Sumner SCJ, Bahman A, Williams CC. Acrylamide, Metabolism, Distribution, & Hemoglobin Adducts in Male F344 Rats and B6C3F1 Mice Following Inhalation Exposure and Distribution and Hemoglobin Adducts Following Dermal Application to F344 Rats. Res. Triangle Park 2001; NC: CIIT.

38. Tanaka H, Takahashi S, Oki J. Developmental regulation of spinal motorneurons by monoaminergic nerve fibers. J Periph Nerv Sys 1997; 2: 323-332.

39. Tracey DJ. Ascending and descending pathways in the spinal cord. In: Paxinos G, editor. The rat nervous system. Academic Press pp 689-704, New York 1995.

40. Tyl R, Marr C, Myers B, Ross P, Friedman A. Relationship between acrylamide reproductive and neurotoxicity in male rats. Rep Toxicol 2000; 14: 147-57.

41. Uphouse L, Nemeroff CB, Mason G, Prange AJ, Bondy SC. Interactions between "handling" and acrylamide on endocrine responses in rats. Neurotoxicology 1982: 3(1): 121-125.

42. Warr T, Parry J, Callander R. Methyl vinyl sulphone: a new class of Michael-type genotoxin. Mutat Res 1990; 245: 191-199.

43. Wise LD, Gordon LR, Soper KA, Duchai DM, Morrissey RE. Developmental neurotoxicity evaluation of acrylamide in Sprague –Dawley rats. Neurotoxicol Teratol 1995; 17: 189-198.

44. Yousef MI, El-Demerdash FM. Acrylamide-induced oxidative stress and biochemical perturbations in rats. Toxicology 2006; 219: 133-141.

45. Zhang L, Gavin T, Barber DS, LoPachin RM. Role of the Nrf2-ARE pathway in acrylamide neurotoxicity. Toxicol Lett 2011; 10;205(1): 1–7.

8/12/2013